Journal of Russian Laser Research, Volume 33, Number 4, July, 2012

TWO COUPLED OSCILLATORS IN THE FORM OF A FREQUENCY CONVERTER IN INTERACTION WITH A SINGLE ATOM VIA TWO-PHOTON PROCESSES

M. Sebawe Abdalla[1*] and E. M. Khalil[2,3]

[1] *Mathematics Department, College of Science*
King Saud University
P.O. Box 2455, Riyadh 11451, Saudi Arabia
[2] *Mathematics Department, College of Science*
Hail University, Saudi Arabia
[3] *Mathematics Department, Faculty of Science*
Al-Azher University
Nassr City 11884, Cairo, Egypt

*Corresponding author e-mail: m.sebaweh @ physics.org

Abstract

We consider the problem of a two-level atom with degenerate two-photon transitions interacting with a single-mode radiation field in the presence of a parametric frequency-converter term. A Hamiltonian representing such a system contains three time-dependent coupling parameters. We obtain an exact solution of the wave function in the Schrödinger picture, using the canonical transform and under a certain choice of the coupling parameters. We use the results obtained to discuss the atomic inversion as well as the linear entropy in addition to both the variance and entropy squeezing. We show that the system at a certain time is sensitive to variations in both the detuning parameter Δ and the ratio of the coupling parameter g.

Keywords: linear entropy, atomic squeezing, entanglement, Jaynes–Cummings model.

1. Introduction

Doubtless, the Jaynes–Cummings model (JCM), which comprises a single two-level atom interacting with a single cavity mode of the electromagnetic field [1] together with its various modifications and generalizations plays an important role in the field of quantum optics [2–6]. The model can be regarded as the richest source for the description of nonclassical phenomena. For example, the vacuum-field Rabi splitting has been predicted theoretically and corroborated experimentally. In the meantime, we can see that the two-photon interaction of a single two-level atom with the quantized electromagnetic field has been the subject of considerable study. This is due to its importance in revealing the nonclassical properties of multiphoton transitions of atoms and the experimental development of a two-photon micromaser.

Manuscript submitted by the authors in English on July 11, 2012.

 1071-2836/12/3304-0336

Considerable attention has been paid to the nondegenerate two-photon JCM for realizing a two-mode two-photon laser [7–11]. This attention arose after Gauthier et al. constructed the first single-mode two-photon laser based on dressed atomic states [12]. In this context, we may mention that in the two-photon processes the intensity-dependent effects must be taken into account; so the authors of [13, 14] generalized the intensity-dependent JCM to a two-mode cavity field with a two-photon process and studied its dynamic properties.

On the other hand, the physical spectrum defined by Eberly and Wodkiewicz has been studied widely because much of the information obtained in experiments comes in the form of spectral data [15]. The cavity–field spectra of the two-photon JCM [16], the nondegenerate two-photon JCM [17], and the two-atom–two-photon JCM [18–21] were also studied. However, the effects of the parametric frequency-converter property of the coupling parameter were not taken into consideration.

Recently, the problem of the nonlinear interaction between two electromagnetic-field modes and a two-level atom was considered [22]. Under the assumption that the two-level atom interacts with each mode separately as well as with the two modes nonlinearly, the effects of the degenerate and nondegenerate processes were considered. In the present work, we introduce a Hamiltonian model, which describes the interaction between a two-level atom and a quantum system, consists of the frequency-converter model in the presence of the second-harmonic generation (degenerate two-photon process) [23]. The Hamiltonian that describes such a kind of interactions is given by

$$\frac{\hat{H}(t)}{\hbar} = \sum_{i=1}^{2} \omega_i \hat{a}_i^{\dagger}\hat{a}_i + \frac{\omega_0}{2}\hat{\sigma}_z + \sum_{i=1}^{2}\left[\left(\lambda_i(t)\hat{a}_i^2 + \lambda_i^*(t)\hat{a}_i^{\dagger 2}\right) + \left(\lambda_3(t)\hat{a}_1\hat{a}_2^{\dagger} + \text{h.c.}\right)\right]\hat{\sigma}_x, \tag{1}$$

where $\lambda_i(t),\ i = 1, 2$ are the time-dependent coupling response of the second-harmonic generation and $\lambda_3(t)$ is the time-dependent coupling-parameter response of the frequency-converter term. These coupling parameters are given as

$$\lambda_j(t) = g_j \exp[i(2\bar{\omega}_j t + \phi_j)], \quad j = 1, 2, \qquad \lambda_3(t) = g_3 \exp[i(\bar{\omega}_1 - \bar{\omega}_2)t + \phi_i)], \tag{2}$$

where $\bar{\omega}_i$ and ϕ_i $(i = 1, 2)$ are the frequencies and phase pumps, respectively, and $\omega_i, i = 1, 2$ are the free field frequencies, ω_0 is the atomic-system frequency, and the operators $\hat{a}_i^{\dagger}$ $(\hat{a}_i)$ $(i = 1, 2)$ are the creation and annihilation operators that satisfy the commutation relation $[\hat{a}_i, \hat{a}_j^{\dagger}] = \delta_{ij}$, with $\delta_{ij} = 1$ when $i = j$ and zero, otherwise. The operators $\hat{\sigma}_x = (\hat{\sigma}_+ + \hat{\sigma}_-)$ and $\hat{\sigma}_z$ are the usual Pauli matrices that follow the relations

$$[\hat{\sigma}_z, \hat{\sigma}_\pm] = \pm 2\hat{\sigma}_\pm, \qquad [\hat{\sigma}_+, \hat{\sigma}_-] = \hat{\sigma}_z. \tag{3}$$

Note that the existence of the frequency-converter term in Hamiltonian (1) indicates an exchange between the energy of the fields. This is in contrast to the previous work [22] where the existence of the parametric-amplifier term leads to amplifying the energy between the field modes.

As one can see, Hamiltonian (1) describes a time-dependent nonlinear quantum system that includes three coupling parameters. This means that it is not an easy task to deal with such a Hamiltonian. Therefore, to avoid this complication, one must introduce a certain canonical transform to remove at least the time factor from the system. This is seen in Sec. 2 where we also introduce the exact solution for the wave function. In Sec. 3, we discuss the atomic inversion, and in Sec. 4 we consider the linear entropy of the system. In Sec. 5, we present the variance and entropy squeezing, while in Sec. 6 we give our conclusions.

2. The Wave Function

Our main purpose in this section is to introduce the exact solution of the wave function from which we are able to discuss some statistical properties of the present system. To reach this goal, we have first to remove the time-dependent factors from Hamiltonian (1). For this reason, we introduce the operators $\hat{A}_i(t) = \hat{a}_i(t)\exp[i(\bar{\omega}_i t + \phi_i/2)]$. In this case and after applying the canonical transform to Hamiltonian (1), it becomes time-independent and takes the form

$$\frac{\hat{H}}{\hbar} = \sum_{i=1}^{2} \Delta_i \hat{A}_i^\dagger \hat{A}_i + \frac{\omega_0}{2}\hat{\sigma}_z + \sum_{i=1}^{2}[g_i(\hat{A}_i^2 + \hat{A}_i^{\dagger 2}) + g_3(\hat{A}_1\hat{A}_2^\dagger + \text{h.c.})]\hat{\sigma}_x, \tag{4}$$

where $\Delta_i = (\omega_i - \bar{\omega}_i),\ i = 1, 2$.

Even though we have managed to remove the time-dependent factor from the Hamiltonian, nevertheless, the system is still complicated to deal with it. Therefore, we introduce the transform

$$\hat{A}_1 = \hat{B}_1\cosh\vartheta - \hat{B}_2^\dagger\sinh\vartheta, \qquad \hat{A}_2 = \hat{B}_2\cosh\vartheta - \hat{B}_1^\dagger\sinh\vartheta, \tag{5}$$

from which Hamiltonian (4) takes the form

$$\frac{\hat{H}}{\hbar} = \Delta_1(\hat{B}_1^\dagger\hat{B}_1 - \hat{B}_2^\dagger\hat{B}_2) + \frac{\omega_0}{2}\hat{\sigma}_z + \sum_{i=1}^{2}\mu_i(\hat{B}_i^2\hat{\sigma}_+ + \hat{B}_i^{\dagger 2}\hat{\sigma}_-), \tag{6}$$

where we applied the rotating-wave approximation and considered $\omega_1 + \omega_2 = \bar{\omega}_1 + \bar{\omega}_2$. Note that in the above equation we defined

$$\mu_1 = g_1\cosh^2\vartheta + g_2\sinh^2\vartheta - g_3\sinh 2\vartheta, \qquad \mu_2 = g_2\cosh^2\vartheta + g_1\sinh^2\vartheta - g_3\sinh 2\vartheta, \tag{7}$$

where

$$\vartheta = \frac{1}{2}\tanh^{-1}\left(\frac{2g_3}{g_1 + g_2}\right). \tag{8}$$

Now Hamiltonian (6) is the usual two-mode JCM in the presence of two photons. Within the framework of this model, it is still difficult to find its wave function or to obtain its time-dependent dynamic operators. However, if we consider the case where $g_3 = \sqrt{g_1 g_2}$, we find $\mu_2 = 0$ and, consequently, the Hamiltonian reduces to the form

$$\frac{\hat{H}}{\hbar} = \Delta_1\hat{B}_1^\dagger\hat{B}_1 + \frac{\omega_0}{2}\hat{\sigma}_z + \mu_1(\hat{B}_1^2\hat{\sigma}_+ + \hat{B}_1^{\dagger 2}\hat{\sigma}_-). \tag{9}$$

Here we may point out that the restrictive condition $g_3 = \sqrt{g_1 g_2}$ may be regarded as an integrability condition under which we are able to consider the system dynamics analytically.

As we see, the system is converted to the interaction between the two-level atom and two-photon single field. Therefore, we are in a position to derive the wave function for the present system. To do this, we employ the equations of motion in the Heisenberg picture to get some invariants from which we are able to reach our aim. The equations of motion are

$$\begin{aligned}
\frac{d\hat{B}_1}{dt} &= -i\Delta_1\hat{B}_1 - 2i\mu_1\hat{B}_1^\dagger\hat{\sigma}_-, \qquad \frac{d\hat{B}_1^\dagger}{dt} = i\Delta_1\hat{B}_1^\dagger + 2i\mu_1\hat{B}_1\hat{\sigma}_+, \\
\frac{d\hat{\sigma}_-}{dt} &= -i\omega_0\hat{\sigma}_- + 2i\mu_1\hat{B}_1^2\hat{\sigma}_z, \qquad \frac{d\hat{\sigma}_+}{dt} = i\omega_0\hat{\sigma}_+ - 2i\mu_1\hat{B}_1^{\dagger 2}\hat{\sigma}_z, \\
\frac{d\hat{\sigma}_z}{dt} &= -2i\mu_1(\hat{B}_1^2\hat{\sigma}_+ - \hat{B}_1^{\dagger 2}\hat{\sigma}_-).
\end{aligned} \tag{10}$$

After straightforward calculations, we have $\hat{H}/\hbar = \Delta_1\hat{N} + \hat{C}$, where

$$\hat{C} = \frac{\Delta}{2}\hat{\sigma}_z + \mu_1(\hat{B}_1^2\hat{\sigma}_+ + \hat{B}_1^{\dagger 2}\hat{\sigma}_-), \qquad \hat{N} = \hat{m} + \hat{\sigma}_z, \tag{11}$$

and $\hat{m} = \hat{B}_1^\dagger\hat{B}_1$, while

$$\Delta = \omega_0 - 2\Delta_1, \qquad \mu_1 = \frac{1-g}{1+g}, \qquad g = \frac{g_2}{g_1}. \tag{12}$$

Now suppose that the field was initially in the coherent state $|\psi\rangle_f$, such that

$$\begin{aligned} |\psi\rangle_f &= \sum_{m=0}^{\infty} Q_m\,|m\rangle, \qquad Q_m = K\frac{\tanh^{m/2}\vartheta}{\sqrt{2^m m!}}H_m(\beta/\sqrt{\sinh 2\vartheta}), \\ K^{-2} &= \sum_{m=0}^{\infty}\frac{1}{2^m m!}|H_m(\beta/\sqrt{\sinh 2\vartheta})|^2|\tanh\vartheta|^m, \end{aligned} \tag{13}$$

where β is the coherent-state complex parameter and $H_m(\beta/\sqrt{\sinh 2\vartheta})$ are the Hermite polynomials. In the meantime, we assume that the atom is initially in the atomic coherent state $|\psi\rangle_a$, and this state can be constructed to take the form

$$|\psi\rangle_a = \cos\theta|+\rangle + e^{i\phi}\sin\theta|-\rangle, \tag{14}$$

where $|+\rangle$ and $|-\rangle$ are the excited and ground states, while ϕ is a relative phase angle and θ is the coherence angle. The wave function for the system at $t = 0$ is now given by $|\psi(0)\rangle = |\psi\rangle_f \otimes |\psi\rangle_a$. Using the above result, we can write the wave function at $t > 0$ as

$$|\psi(t)\rangle = \sum_{m=0}^{\infty} Q_m[\hat{F}(g,m,t)|m,+\rangle + \hat{G}(g,m,t)|m,-\rangle], \tag{15}$$

where $\hat{F}(g,m,t)$ and $\hat{G}(g,m,t)$ are given by

$$\begin{aligned} \hat{F}(g,m,t) &= e^{-it\Delta_1(\hat{B}_1^\dagger\hat{B}_1+1/2)}\left\{\cos\theta\left[\cos\hat{\nu}_1 t - i\frac{\Delta}{2}\frac{\sin\hat{\nu}_1 t}{\hat{\nu}_1}\right] + \mu_1 e^{i\phi}\sin\theta\frac{\sin\hat{\nu}_1 t}{\hat{\nu}_1}\hat{B}_1^2\right\}, \\ \hat{G}(g,m,t) &= e^{-it\Delta_1(\hat{B}_1^\dagger\hat{B}_1-1/2)}\left\{e^{i\phi}\sin\theta\left[\cos\hat{\nu}_2 t + i\frac{\Delta}{2}\frac{\sin\hat{\nu}_2 t}{\hat{\nu}_2}\right] + \mu_1\cos\theta\frac{\sin\hat{\nu}_2 t}{\hat{\nu}_2}\hat{B}_1^{\dagger 2}\right\}, \end{aligned} \tag{16}$$

with

$$\hat{\nu}_1^2 = \frac{\Delta^2}{4} + \mu_1^2\hat{B}_1^2\hat{B}_1^{2\dagger}, \qquad \hat{\nu}_2^2 = \frac{\Delta^2}{4} + \mu_1^2\hat{B}_1^{2\dagger}\hat{B}_1^2. \tag{17}$$

Using the above results, we are able to discuss some statistical properties of the present model. In the next section, we concentrate on the behavior of the atomic inversion.

3. The Atomic Inversion

In this section, we consider the atomic inversion to see the effects of the second-harmonic generation and the parametric frequency converter on the system. It is well known that the atomic inversion is the

difference between the probability of finding the atom in the excited state and the probability of finding the atom in the ground state. Therefore, if we assume that the atom starts in its excited state, we can show that the atomic inversion $W(t, g)$ reads

$$W(g,t) = \sum_{m=0}^{\infty} |Q_m|^2 (|\langle \hat{F}(g,m,t)\rangle|^2 - |\langle \hat{G}(g,m,t)\rangle|^2). \tag{18}$$

In fact, the above equation allows us to observe the atomic behavior and to determine whether the atom is in its excited state or in its ground state. Furthermore, it would help us to see when the atom is in the maximum state, where the probabilities of finding the atom in the excited state and in the ground state are equal. Usually the numerical investigations concentrate on the time variation. However, in this study we fix time and examine the system behavior with respect to the coupling-parameter ratio g, taking into account that the atom was initially in the excited state and the field was prepared in the squeezed state. We consider the initial mean photon number $\bar{m} = 25$.

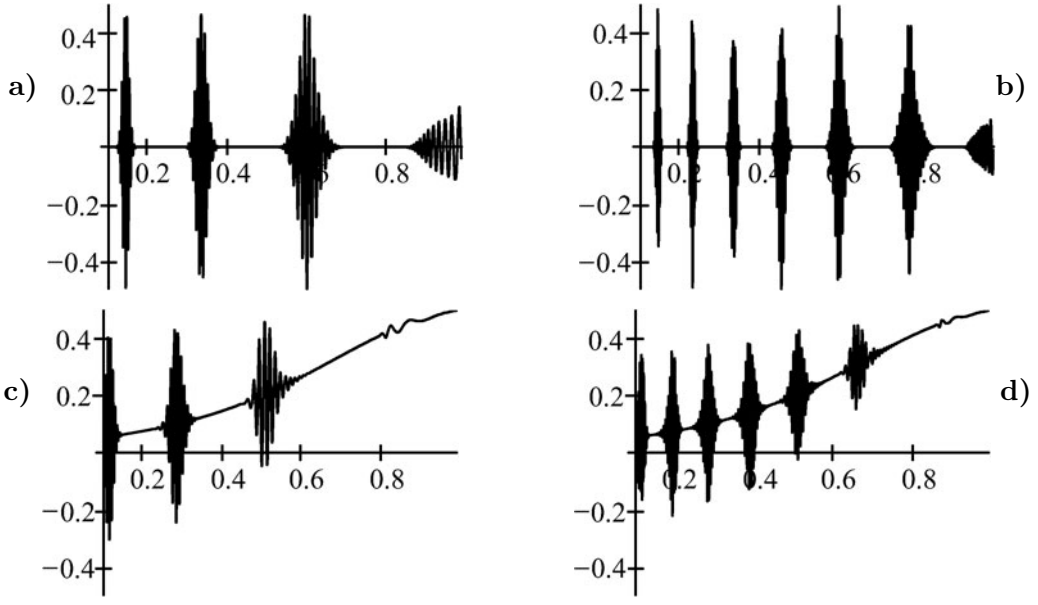

Fig. 1. The evolution of the atomic inversion with the initial mean photon number $\bar{m} = 25$. The atom started from the excited state ($\theta = 0$), where $\Delta = 0$ and $t = 4\pi$ (a), $\Delta = 0$ and $t = 8\pi$ (b), $\Delta = 15$ and $t = 4\pi$ (c), and $\Delta = 15$ and $t = 8\pi$ (d).

In Fig. 1 a and b, we consider the resonance case where $\Delta = 0$ for two different periods of time $t = 4\pi$ and 8π. In the first case, we can see that the function starts with a small domain of the collapse, which is followed by a small domain of the revival. However, the second domain of the revival occurs after a large value of g (compared with the first domain), where the collapse domain can be seen, Fig. 1 a. In this case, we also observe that a partial flipping from the upper to the lower state occurs, and the collapses and revivals of the atomic inversion occur regularly. This is in addition to the maximum state occurring at the collapse intervals. Further, we note that the value of g increases as the domains of both collapses and revivals increase. This means that there is a strong interaction between the atom and the fields. This behavior is repeated during the fixed period of time under consideration. When

time increases, $t = 8\pi$, the function exhibits the same behavior, but with an increase in the number of the collapse and revival domains. Also, more interference between the patterns during the fluctuations within the revival domains can be observed; see Fig. 1 b. In this case, the function shows an decrease in the amplitude of the oscillations within the revival domains for a small value of g; however, it increases as the coupling-parameter ratio g increases.

The situation is different if we take into account the detuning parameter (off-resonance case) and set $\Delta = 15$. In this case and for $t = 4\pi$, the behavior of the function changes and its value shifts up as usually seen in the JCM case. This means that the energy is stored in the atomic system and does not reach the ground state for higher values of the coupling-parameter ratio g as shown in Fig. 1 c. Also we note that the function starts in the revival domain with fluctuations occurring between -0.35 and 0.4. We observe that the collapses and revivals occur at short intervals. This gets more pronounced when we consider the case $t = 8\pi$, where the function demonstrates a behavior similar to that of $t = 4\pi$; see Fig. 1 d. However, we can see an increase in the number of both collapses and revivals. This is in addition to a decrease in the range of the function fluctuations. Finally, we emphasis that with increase in the value of the coupling-parameter ratio g, there exists an inhibition of the energy between the atom and the optical field, provided the detuning parameter $\Delta \neq 0$. In what follows, we consider the degree of entanglement by employing the linear entropy. This is seen in the next section.

4. Linear Entropy

Recently, most applications in quantum-information technology is based on the entanglement. As examples, we mention quantum computation [24], quantum cryptography [25, 26], quantum teleportation [27, 28], and many other applications [29–32]. On the other hand, the disentanglement of the two quantum systems provides interesting applications, e.g., in preparation of atomic states through interacting quantum systems to determine the cavity field; see, for example, [33–35]. In the meantime, the purity $P(g,t)$ (say) can be used as a good tool to give information on the entanglement of the system components. Also we can see that the purity parameter assumes a relevant role in quantum information where the effective fidelities of protocols depend critically on the purity of the information-carrier states. Furthermore, during the consideration of the connection between generalized uncertainty relations and optical tomograms, it was shown that the purity of the states can be retrieved by statistical analysis of the homodyne data, see [36]. For these mentioned reasons, we discuss the purity of the system under consideration. The purity of the field state can be determined from the quantity

$$P(t) = 1 - \mathrm{Tr}\,[\hat{\rho}_f^2(t)], \tag{19}$$

where $\hat{\rho}_f(t) = \mathrm{Tr}\,\hat{\rho}_a(t)$ is the field reduced density matrix. The density matrix $\hat{\rho}(t)$ can be obtained from Eq. (15) and takes the form

$$\hat{\rho}(t) = \sum_{m,n=0}^{\infty} Q_m Q_n^* \left[F|m,+\rangle\langle+,n|F^* + G|m,-\rangle\langle+,n|F^* + F|m,+\rangle\langle-,n|G^* + G|m,+\rangle\langle-,n|G^*\right]. \tag{20}$$

The necessary and sufficient conditions for the ensemble to be described in terms of a pure state is $\mathrm{Tr}\,[\hat{\rho}_f^2(g,t)] = 1$. However, for the case where $\mathrm{Tr}\,[\rho_f^2(t)] < 1$, the field is in a statistical mixture of

the states, while for a two-level system the maximum mixed ensemble corresponds to $\mathrm{Tr}\,[\rho_f^2(t)] = 1/2$. Analytic conclusions about the system's state-vector dynamics and the atom–field entanglement can be verified through examining the linear entropy. The linear entropy of reduced atomic (or field) density matrix can serve for evaluating the degree of entanglement of systems consisting of two subsystems prepared in pure states. The linear entropy of reduced atomic density matrix for the considered system has the form

$$P(g,t) = \left(1 - X_1^2(g,t) - X_2^2(g,t) - 2|X_3(g,t)|^2\right), \tag{21}$$

where

$$\begin{aligned} X_1(g,t) &= \sum_{m=0}^{\infty} |Q_m|^2 |F\,(g,m,t)\,|^2, \qquad X_2(g,t) = \sum_{m=0}^{\infty} |Q_m|^2 |G\,(g,m,t)\,|^2, \\ X_3(g,t) &= \sum_{m=0}^{\infty} Q_{m+2} Q_m^* F\,(g,m+2,t)\,G^*\,(g,m,t)\,. \end{aligned} \tag{22}$$

Now we use the above equations to analyze and discuss the linear entropy.

Due to the complicated form of the equations, we must use numerical computations. For this, we plot the function $P(g,t)$ against the coupling-parameter ratio g for a fixed time, baring in mind that the field is prepared in the squeezed state and the atom is initially prepared in the excited state. In Fig. 2, we show the evolution of the linear entropy for four different cases — the first two cases correspond to $t = 2\pi$ and 4π and $\Delta = 0$, while the second two cases correspond to $t = 2\pi$ and 4π and $\Delta = 15$. We have fixed the value of of the initial mean photon number, $\bar{m} = 25$.

When we consider the case $t = 2\pi$ in the absence of detuning ($\Delta = 0$), the function fluctuates between 0 and 0.5, where partial entanglement can be seen. However, at a small value of the coupling-parameter ratio $g \simeq 0.1$, the function demonstrates a weak entanglement where the interaction between the field and the atom is almost disentangled; see Fig. 2 a. In the meantime, we can also see a strong entanglement at different values of g. However, the number of the intervals in which the strong entanglement occurs is greater than the number of the intervals in which the weak entanglement occurs. A similar behavior is repeated for the case $t = 4\pi$ but at $g \simeq 0.2$. In this case, we can also see more fluctuations compared with the previous case within the same range of g. Furthermore, we observe that an increase in the coupling-parameter ratio g leads to an increase in the minimum values of the linear entropy; see Fig. 2 b.

Now we turn our attention to the nonresonance case ($\Delta = 15,\ t = 4\pi$); here the behavior of the linear entropy is strongly affected. In this case, the minimum of the function increases, and its minimum decreases, where the partial entanglement can be seen. This means that the field is in a mixed state, but its maximum is not reached. However, the function shows disentanglement when the coupling-parameter ratio $g = 1$, which corresponds to $\mu_1 = 0$. In this particular case, the interaction between the atom and the field vanishes completely, as in Fig. 2 c. When time increases, $t = 8\pi$, more irregular fluctuations with interference between the patterns can be seen. This, in addition to an increase in the maximum value of the function, provides an increase in its minimum value where the entanglement appears more pronounced. However, the function displays disentanglement at $g = 1$ for the same reason previously mentioned; see Fig. 2 d.

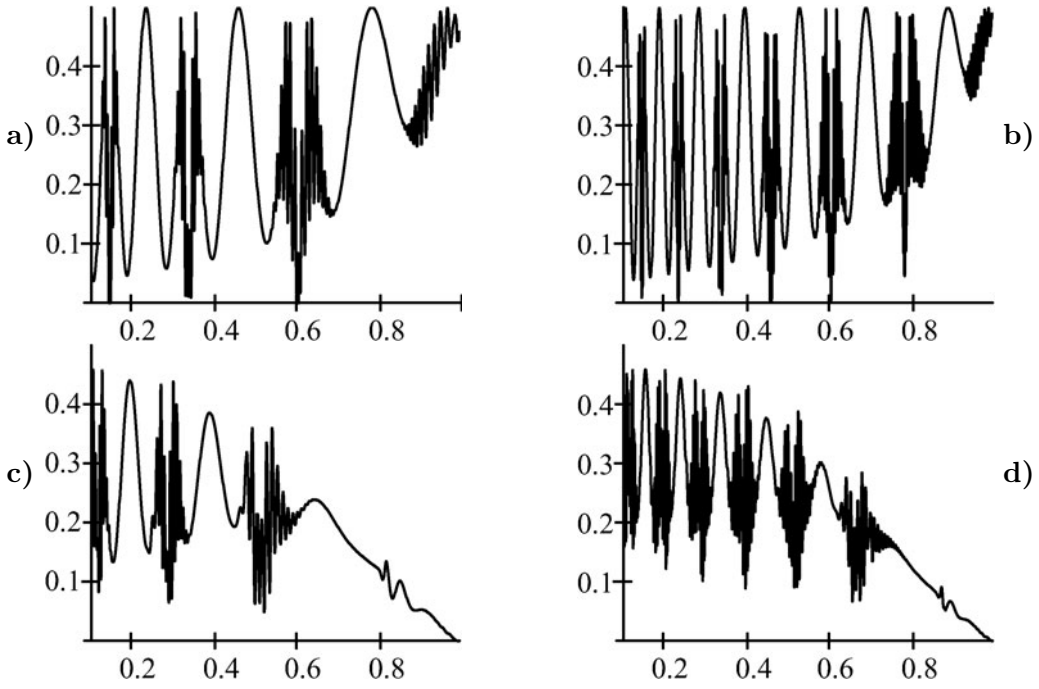

Fig. 2. The time evolution of the linear entropy as a function of the coupling-parameter ratio g (the other parameters are the same as in Fig. 1).

5. The Phenomenon of Squeezing

We devote this section to a discussion of the variance squeezing as well as the entropy squeezing in order to see the effect of the combination between the frequency-converter term and the second-harmonic-generation term in the system of equations for the quantum system. This will be seen in Sects. 5.1 and 5.2.

5.1. Variance Squeezing (Atomic Squeezing)

Recently the arguments for using the entropic uncertainty relations for the two-level system rather than the Heisenberg uncertainty relations to investigate quantum fluctuations were discussed in [37, 38]. In quantum-mechanical system with two physical observables represented by the Hermitian operators $\hat{A}$ and $\hat{B}$ satisfying the commutation relation $[\hat{A}, \hat{B}] = i\hat{C}$, one can write the Heisenberg uncertainty relation in the form

$$\langle(\Delta\hat{A})^2\rangle\langle(\Delta\hat{B})^2\rangle \geq \frac{1}{4}|\langle\hat{C}\rangle|^2, \tag{23}$$

where $\langle(\Delta\hat{Q})^2\rangle = \langle\hat{Q}^2\rangle - \langle\hat{Q}\rangle^2$. Consequently, the uncertainty relation for a two-level atom characterized by the Pauli operators $\hat{S}_x$, $\hat{S}_y$, and $\hat{S}_z$, satisfying the commutation relations $[\hat{S}_x, \hat{S}_y] = 2i\hat{S}_z$, can also be written as $\Delta\hat{S}_x\Delta\hat{S}_y \geq |\langle\hat{S}_z\rangle|$. Fluctuations in the component $\hat{S}_\gamma$ of the atomic dipole are said to be squeezed if $\hat{S}_\gamma$ satisfies the condition

$$V(\hat{S}_\gamma) = (\Delta\hat{S}_\gamma - \sqrt{|\langle\hat{S}_z\rangle|}) < 0, \qquad \gamma = x \text{ or } y. \tag{24}$$

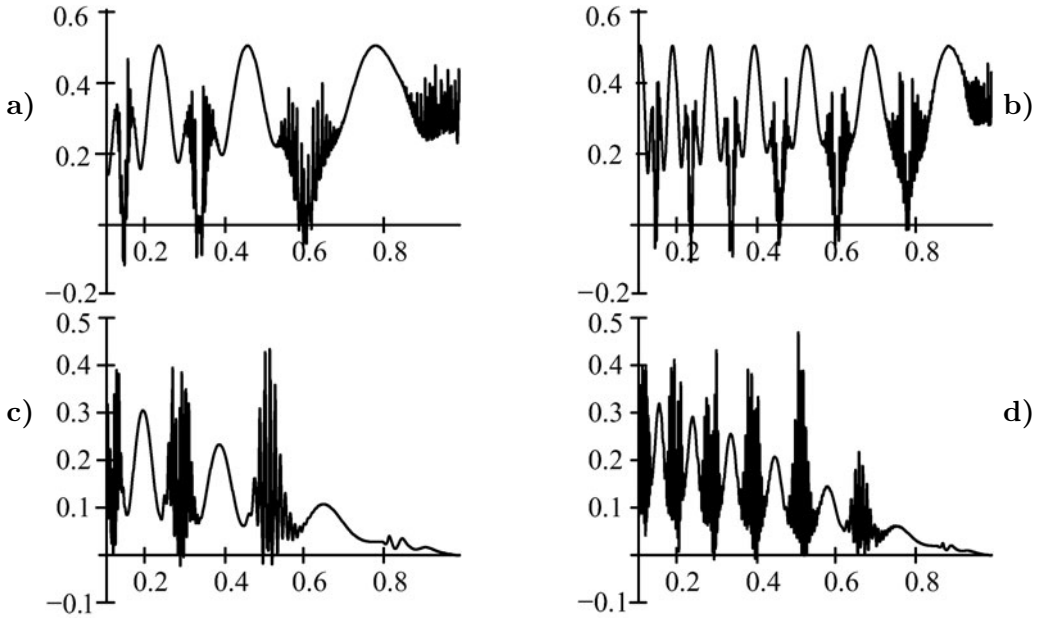

Fig. 3. The variance squeezing V_x against the coupling-parameter ratio g for $\Delta = 0$ and $t = 4\pi$ (a), $\Delta = 0$ and $t = 8\pi$ (b), $\Delta = 15$ and $t = 4\pi$ (c), and $\Delta = 15$ and $t = 8\pi$ (d).

Now we will discuss the variance squeezing.

In our computation program, we have noted that the squeezing phenomenon occurs only in the first quadrature $V_x(g)$ and is absent in the second quadrature $V_y(g)$ for all values of the considered region of the coupling-parameter ratio g. Therefore, we concentrate on the squeezing in the quadrature $V_x(g)$ and plot the function against the coupling-parameter ratio g for different values of the detuning parameter Δ and time t.

In our examination, we consider the same values of the parameters as we took for the atomic inversion and the linear entropy. For example, we examine the system at the exact resonance, where $\Delta = 0$ for two different values of time $t = 4\pi$ and 8π. For $t = 4\pi$, the function shows a periodical behavior and the squeezing can be seen at three different values of g within the considered region (Fig. 3 a). The maximum squeezing in this case occurs around $g \sim 0.1$ and reaches the value -0.12. However, when time increases, $t = 8\pi$, the squeezing occurs more slowly than in the previous case; here the function shows squeezing around $g \sim 0.23$ and reaches the value -0.1. Furthermore, the function in this case shows more periods of the squeezing compared with the case where $t = 4\pi$, see Fig. 3 b. On the other hand, when the detuning parameter is taken into account and we set $\Delta = 15$ and $t = 4\pi$, the function shows a drastic reduction not only in its maximum but also in its minimum, which leads to a decrease in the amount of squeezing compared with the resonance case, see Fig. 3 c. A similar behavior can be seen when time increases, $t = 8\pi$, where the maximum of the function decreases and it exhibits more fluctuations. In the meantime, a small amount of squeezing starts to be seen after $g = 0.2$ (Fig. 3 d).

5.2. The Entropy Squeezing

The second task of this section is to discuss the entropy squeezing. As is well known, the concept of quantum information theory depends on the entropy. Therefore, the use of the entropy squeezing would give us more information on the quantum system under consideration. In an even N-dimensional Hilbert space, the inequality [39–42]

$$\sum_{r=0}^{N+1} H(\hat{S}_\beta) \geq [(N/2)\ln(N/2) + (1+N/2)\ln(1+N/2)] \tag{25}$$

takes place, where $H(\hat{S}_\beta)$ represents the Shannon information entropy of the variable $\hat{S}_\beta$. This, in fact, can be used to describe the optimum entropic uncertainty relation for sets of $(N+1)$ complementary observables with nondegenerate eigenvalues. The corresponding Shannon information entropies are defined by

$$H(\hat{S}_\beta) = -\sum_{j=1}^{N} P_j(\hat{S}_\beta)\ln P_j(\hat{S}_\beta), \qquad \beta = x, y, z, \tag{26}$$

where $P_j(\hat{S}_\beta)$ are the probability distributions for N possible outcomes of measurements of the operator $\hat{S}_\beta$. Therefore, to obtain the information entropies of the atomic operators $\hat{S}_\beta$ for a two-level atom with $N = 2$, we use the expression

$$H(S_\beta) = -\frac{1}{2}\left\{(1+\langle\hat{S}_\beta\rangle)\ln\left[\frac{1}{2}(1+\langle\hat{S}_\beta\rangle)\right] + (1-\langle\hat{S}_\beta\rangle)\ln\left[\frac{1}{2}(1-\langle\hat{S}_\beta\rangle)\right]\right\}. \tag{27}$$

Doubtless, the uncertainty relation for the entropy of any quantum system, which contains the interaction with a two-level atom, can be used as a general criterion for the squeezing of an atom (spinor).

Now, if we define $\delta H(\hat{S}_\beta) = \exp[H(\hat{S}_\beta)]$, then for a two-level atom where $N = 2$, we have $1 \leq \delta H(\hat{S}_\beta) \leq 2$; in this case, the information entropies of the operators $\hat{S}_\beta$ and $\beta = x, y, z$ satisfy the inequality

$$\delta H(\hat{S}_x)\delta H(\hat{S}_y)\delta H(\hat{S}_z) \geq 4. \tag{28}$$

In this context, we refer to [43] where a review of the probability representation of quantum mechanics is presented along with the discussion of experimental possibilities to check the uncertainty relations for the position and momentum [44, 45], as well as the entropic uncertainty relation [46]. This may open the door for more applications in the near future.

On the other hand, if we consider $\delta H(\hat{S}_\beta) = 1$, then the atom will be in the pure state, while the atom will be in a completely mixed state if $\delta H(\hat{S}_\beta) = 2$. The quantities $\delta H(\hat{S}_x)$ and $\delta H(\hat{S}_y)$ are nothing else but quantities measuring uncertainties of the atomic polarization components $\hat{S}_x$ and $\hat{S}_y$, respectively. Then it is clear from the entropic uncertainty relation (25) that it is impossible to have simultaneously the complete information on the observables $\hat{S}_x$ and $\hat{S}_y$. The atomic squeezing can be defined from the entropic uncertainty relation (28), namely, the entropy squeezing. The fluctuations in the components $\hat{S}_\beta$ ($\beta = x$ or y) of the atomic dipole are said to be squeezed in entropy if the information entropy $H(\hat{S}_\beta)$ of $\hat{S}_\beta$ satisfies the condition

$$E(\hat{S}_\beta) = (\delta H(\hat{S}_\beta) - \frac{2}{\sqrt{|\delta H(\hat{S}_z)|}}) < 0, \qquad \beta = x, y. \tag{29}$$

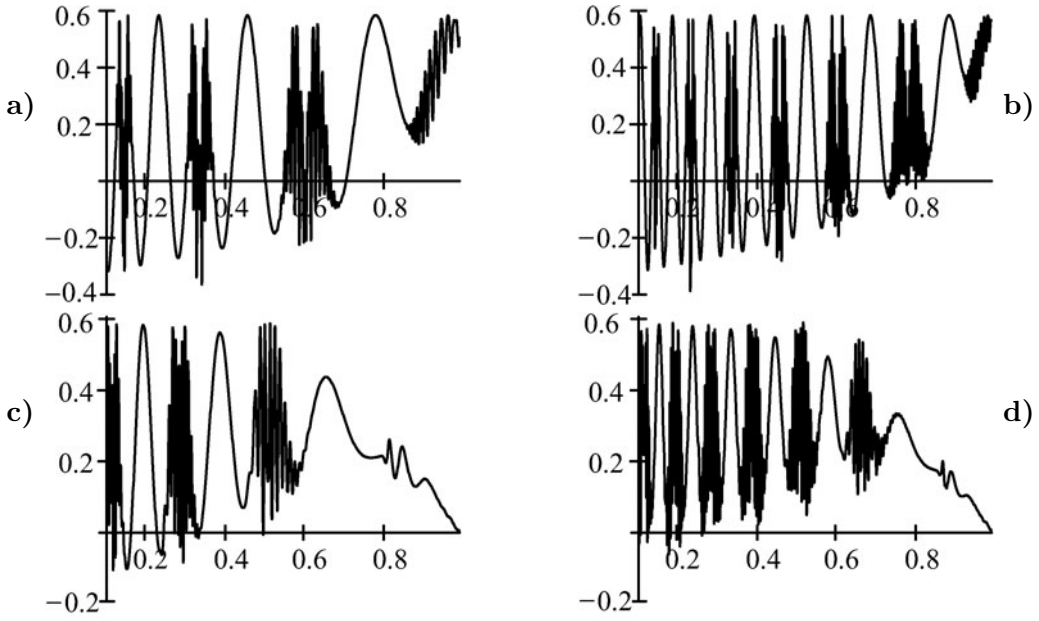

Fig. 4. The entropy squeezing E_x against the coupling-parameter ratio g for $\Delta = 0$ and $t = 4\pi$ (a), $\Delta = 0$ and $t = 8\pi$ (b), $\Delta = 15$ and $t = 4\pi$ (c), and $\Delta = 15$ and $t = 8\pi$ (d).

To obtain the Shannon information entropies of the atomic operators for the system under study, we can use the reduced atomic density operator $\hat{\rho}(t)$. Consequently, Eq. (27) can be written in the form

$$H(S_\alpha) = -\frac{1}{2}[\rho_\alpha(g)+1]\ln\left[\frac{1}{2}[\rho_\alpha(g)+1]\right] - \frac{1}{2}[1-\rho_\alpha(g)]\ln\left[\frac{1}{2}[1-\rho_\alpha(g)]\right], \tag{30}$$

where $\alpha = x, y, z$ and $\rho_\alpha(g) = \langle\psi(0)|\hat{\rho}_\alpha(g)|\psi(0)\rangle$ is the time-dependent density matrix. Straightforward calculations give us the expressions

$$\begin{aligned} \rho_x(g,m,t) &= 2\,\mathrm{Re}\left[\langle|F(g,m,t)|G(g,m,t)\rangle\right], \qquad \rho_y(g,m,t) = 2\,\mathrm{Im}\left[\langle|F(g,m,t)|G(g,m,t)\rangle\right], \\ \rho_z(g,m,t) &= \langle F(g,m,t)|F(g,m,t)\rangle - \langle G(g,m,t)|G(g,m,t)\rangle. \end{aligned} \tag{31}$$

While processing our computation program, we have observed that the squeezing phenomenon occurred only in the quadrature $E(\hat{S}_x)$ and was absent in the quadrature $E(\hat{S}_y)$. Therefore, to discuss the entropy squeezing, we plot Fig. 4 for the functions $E(\hat{S}_x)$ against the coupling ratio g. As before, we consider the field to be initially in the squeezed state, and the atom, in its excited state, $\theta = 0$.

We concentrate on two cases: (1) the exact resonance $\Delta = 0$ and $t = 4\pi$ and 8π, and (2) the off-resonance but also for $t = 4\pi$ and 8π. For the case where $\Delta = 0$ and $t = 4\pi$, the function starts with its maximum squeezing and reaches the value -0.4. However, with increase in the value g the value of squeezing decreases; see Fig. 4 a. In the meantime, the function displays irregular fluctuations with some interference between the patterns. This, besides the squeezing phenomenon, occurred several times during the considered domain of g. With increase in time, the fluctuations of the function increase compared with the previous case, and its minimum decreases, which leads to a reduction in the value of squeezing; see Fig. 4 b. When the detuning takes place ($\Delta = 15$), a considerable reduction is observed in

the function minimum; see Fig. 4 c. This means that the amount of squeezing decreases and consequently the system is sensitive to variations in the detuning parameter. Similar behavior to that of Fig. 4 b is observed in the case where $\Delta = 15$ and $t = 8\pi$. In this case, we see that the minimum value of the quadrature $E(\hat{S}_x)$ decreases in comparison with the case where $\Delta = 0$, see Fig. 4 d. This indicates a decrease in the squeezing within the considered domain of g. Also we note that with increase in g the squeezing decreases. This fact can be interpreted as follows: since $\mu_1 = (1 - g)/(1 + g)$, an increase in the value of g leads to decrease in the value of μ_1. Consequently, the interaction between the atom and the field weakens, which leads to the squeezing death.

6. Conclusions

In this work, we considered the problem of the interaction between the two-level atom and a quantum system. This system Hamiltonian consists of the interacting subsystem terms in the form of the parametric-frequency-converter and the second-harmonic-generation ones. Under a certain transform and with a particular choice of the coupling parameters, we managed to transform the system to the interaction between the single-mode field and the two-level atom. We obtained the solution for the wave function and discussed some statistical properties of this system. For example, we examined the atomic inversion against the coupling-parameter ratio g. We showed that with increase in the coupling-parameter ratio the domains of the collapses and revivals get more pronounced. Furthermore, an increase in time leads to an increase in the number of collapse and revival domains.

We considered the linear entropy where the system under consideration exhibited the strong and weak entanglement domains. These domains are smaller for the weak entanglement in comparison with the strong entanglement. Also we considered the variance squeezing where the squeezing phenomenon is observed in one of the quadratures, namely, $V(\hat{S}_x)$. We noted that the squeezing was pronounced for a small value of the coupling-parameter ratio g; however, it occurs several times for large times. On the other hand, the effect of detuning leads to a decrease in the squeezing. Finally, we examined the entropy squeezing where we reached the same conclusions as to the variance squeezing.

Acknowledgments

The project was supported by the Research enter, College of Science, King Saud University.

References

1. E. T. Jaynes and F. W. Cummings, *IEEE Proc.*, **51**, 89 (1963).
2. M. S. Abdalla, M. M. A. Ahmed, and A-S. F. Obada, *Physica A*, **162,** 215 (1990).
3. M. S. Abdalla, M. M. A. Ahmed, and A-S. F. Obada, *Physica A*, **170,** 393 (1991).
4. M. Abdel-Aty and M. S. Abdalla, *Physica A*, **307**, 437 (2002).
5. M. Abdel-Aty, M. S. Abdalla, and A.-S. F.Obada, *J. Opt. B: Quantum Semiclass. Opt.*, **4,** 134 (2002).
6. M. Abdel-Aty, M. S. Abdalla, and A.-S. F. Obada, *J. Opt. B: Quantum Semiclass. Opt.*, **4,** S133 (2002).
7. A. Wallraff, D. I. Schuster, A. Blais, et al., *Nature*, **431**, 162 (2004).

8. I. Chiorescu, P. Bertet, K. Semba, et al., *Nature*, **431**, 159 (2004).
9. J. Johansson, S. Saito, T. Meno, et al., *Phys. Rev. Lett.*, **96**, 127006 (2006).
10. A. A. Houck, D. I. Schuster, J. M. Gambetta, et al., *Nature*, **449**, 328 (2007).
11. O. Astafiev, K. Inomata, A. O. Niskanen, et al., *Nature*, **449**, 588 (2007).
12. D. J. Gauthier, Q. L. Wu, S. E. Morrin, and T. W. Mossberg, *Phys. Rev. Lett.,* **68**, 464 (1992).
13. B. Buck and C. V. Sukumar, *Phys. Lett. A*, **81**, 132 (1981).
14. A. Napoli and A. Messina, *J. Mod. Opt.*, **43**, 649 (1996).
15. J. H. Eberly and K. Wodkiewcz, *J. Opt. Soc. Am. A*, **67**, 1252 (1977).
16. T. Nasreen and M. S. K. Razmi, *J. Opt. Soc. Am. A*, **10**, 1292 (1993).
17. M. M. Ashraf, *Phys. Rev. A*, **50**, 5116 (1994).
18. Y.-F. Gao, J. Feng, and T.-Q. Song, *Acta Opt. Sinica*, **20**, 1194 (2000).
19. E. M. Khalil, M. S. Abdalla, A.-S. F. Obada, and Jan. Peřina, *J. Opt. Soc. Am. B*, **27**, 266 (2010).
20. M. S. Abdalla, E. M. Khalil, and A.-S. F. Obada, *Ann. Phys.*, **11**, 2554 (2007).
21. E. M. Khalil, M. S. Abdalla, and A.-S. F. Obada, *Ann. Phys.*, **321**, 421 (2006).
22. M. S. Abdalla, A.-S. F. Obada, and M. Abdel-Aty, *J. Phys. B: At. Mol. Opt. Phys.*, **37**, 775 (2004).
23. E. M. Khalil and M. S. Abdalla, *J. Russ. Laser Res.*, **33**, 128 (2012).
24. P. W. Shor, *Phys. Rev. A*, **52**, R2493 (1995).
25. A. K. Ekert, *Phys. Rev. Lett.*, **67**, 661 (1991).
26. A. K. Ekert, J. G. Rarity, P. R. Tapster, and G. M. Palma, *Phys. Rev. Lett.*, **69**, 1293 (1992).
27. C. H. Bennett, G. Brassard, C. Crepeau, et al., *Phys. Rev. Lett.*, **70**, 1895 (1993).
28. C. H. Bennet and S. J. Weisner, *Phys. Rev. Lett.*, **69**, 2881 (1992).
29. S. F. Huelga, C. Macchiavello, T. Pellizzari, et al., *Phys. Rev. Lett.*, **79**, 3865 (1997).
30. S. Bose, V. Vedral, and P. L. Knight, *Phys. Rev. A*, **57**, 822 (1998).
31. M. Murao, M. B. Plenio, S. Popescue, et al., *Phys. Rev. A*, **57**, R4075 (1998).
32. A. Carlson, M. Koashi, and N. Imoto, *Phys. Rev. A*, **59**, 162 (1999).
33. S. J. D. Phoenix and P. L. Knight, *Phys. Rev. A*, **44**, 6023 (1991).
34. S. J. D. Phoenix and P. L. Knight, *Phys. Rev. Lett.*, **66**, 2833 (1991).
35. V. Buźek, H. Moya-Cessa, and P. L. Knight, *Phys. Rev. A*, **45**, 8190 (1992).
36. V. I. Man'ko, G. Marmo, A. Porzio, et al., *Phys. Scr.*, **83**, 045001 (2011).
37. Mao-Fa Fang, Pengzhou, and S. Swain, *J. Mod. Opt.*, **47**, 1043 (2000).
38. E. Majernikova, V. Majernik, and S. Shpyrko, *Eur. J. Phys. B*, **38**, 25 (2004).
39. M. S. Abdalla, E Lashin, and G. Sadiek, *J. Phys. B: At. Mol. Opt. Phys.*, **41**, 015502 (2008).
40. G. Sadiek, E. Lashin, and M. S. Abdalla, *Physica*, **B**, **404**, 1719 (2009).
41. M. S. Abdalla and M. M. A. Ahmed, *Opt. Commun.*, **284**, 1933 (2011).
42. M. S. Abdalla, H. Eleuch, and Jan Peřina, *J. Opt. Soc. Am. B*, **29**, 719 (2012).
43. M. A. Man'ko and V. I. Man'ko, *Found. Phys.*, **41**, 330 (2011).
44. A. Ibort, V. I. Man'ko, G. Marmo, et al., *Phys. Scr.*, **79**, 065013 (2009).
45. V. I. Man'ko, G. Marmo, A. Simoni, and F. Ventriglia, *Adv. Sci. Lett.*, **2**, 517 (2009).
46. S. De Nicola, R. Fedele, M. A. Man'ko, and V. I. Man'ko, *Eur. Phys. J. B*, **52**, 191 (2006).